ISBN: 978-3-95450-227-1 ISSN: 2673-5490 doi:10.18429/JACoW-IPAC2022-MOPOPT058

MACHINE LEARNING TRAINING FOR HOM REDUCTION IN A TESLA-TYPE CRYOMODULE AT FAST*

J. Diaz Cruz[1]†, A. Edelen, J.P. Sikora, B. Jacobson, SLAC, Menlo Park, CA 94720, USA
A. Lumpkin, D. Edstrom, R. Thurman-Keup, FNAL, Batavia, IL 60510, USA
[1]also at University of New Mexico, Albuquerque, NM 87131, USA

Abstract

Low emittance electron beams are of high importance at facilities like the Linac Coherent Light Source II (LCLS-II) at SLAC. Emittance dilution effects due to off-axis beam transport for a TESLA-type cryomodule (CM) have been shown at the Fermilab Accelerator Science and Technology (FAST) facility. The results showed the correlation between the electron beam-induced cavity high-order modes (HOMs) and the Beam Position Monitor (BPM) measurements downstream the CM. Mitigation of emittance dilution can be achieved by reducing the HOM signals. Here, we present a couple of Neural Networks (NN) for bunch-by-bunch mean prediction and standard deviation prediction for BPMs located downstream the CM.

INTRODUCTION

Low emittance electron beams are of high importance in accelerating structures at large facilities like the LCLS-II at SLAC. With a set of experiments performed at FAST, it was shown that off-axis beam transport may result in emittance dilution due to transverse long-range (LRW) and short-range wakefields (SRW) [1, 2]. A set of LRWs known as Higher-Order Modes (HOM) have amplitudes that are proportional to beam offset, charge and coupling impedance (R/Q). Therefore, reducing HOM signals may help to mitigate emittance dilution effects.

In order to further investigate the relation between HOMs and beam offset, a new set of experiments were performed at FAST. This time, two 4-channel HOM detectors were used to measure signals at the upstream (US) and downstream (DS) couplers of 8 superconducting RF (SRF) cavities inside a Tesla-type CM [3]. The new results showed a correlation between the electron beam-induced cavity HOM signal levels and bunch-by-bunch mean and centroid slewing at 11 BPMS located downstream of the CM [4]. In this paper, we evaluate two NN models for bunch-by-bunch mean prediction and centroid slewing prediction based on HOM signals, with the goal of using them for a controller that can drive the steering magnets to minimize beam offset and HOM signals.

* Work supported under contract DE-AC02-76SF00515 with the U.S. Department of Energy.
Work supported by Fermi Research Alliance, LLC under Contract No. DE-AC02-07CH11359 with the U.S. Department of Energy
† dejorge@slac.stanford.edu

EXPERIMENTAL SETUP AND DATA ACQUISITION

The Hardware

The Integrable Optics Test Accelerator (IOTA) at the FAST facility has a unique configuration of two TESLA-type SRF cavities after a photocatode RF gun, followed by an 8-cavity CM, similar to the LCLS-II CMs. Four meters US the CM, there is a set of horizontal and vertical correctors (H/V125) used to steer the electron beam and there are 11 BPMs DS the CM over a 80 m length.

Two 4-channel chassis were built to detect the magnitude of the HOMs at the US and DS couplers of each SRF cavity. Each channel has a 1.3 GHz notch filter to reduce the nominal resonant frequency, a bandpass filter centered at 1.75 GHz with 300 MHz bandwidth to emphasize the main TE111 HOM dipole modes, and a Schottky diode for HOM detection. More details are found in [3].

The Experiment

An electron beam of 50 bunches and 3 MHz bunch repetition rate is produced at the RF gun with an energy of <5 MeV. This bunch pattern repeats at 1 Hz and each repetition is called a ”shot”. After the two capture cavities (CC1 and CC2), the 25 MeV beam is transported to and through the CM with an exit energy of 100 MeV. HOM waveforms and BPM data are capture while steering the beam using the H/V125 corrector magnets, for different values of bunch charge. First, a ”reference” trajectory is found manually by minimizing as many US HOM signals as possible by steering the beam. Then, we capture HOM and BPM data for this reference trajectory and for several values of bunch charge. We then repeat the previous measurements for values of the corrector currents from -1.5 A to 1.5 A in 0.5 A steps.

The Data

An US HOM waveform example for all 8 cavities is shown in Fig. 1. Although several features can be extracted from each of these waveforms (rising time, oscillation frequency, decaying time), we decided to use the peak value as a representative number. Averaging the peak value over 300 shots, the relation between V125 corrector current and HOM signal peaks average is shown in Fig. 2.

BPM average measurements over 300 shots are shown in Fig. 3. Removing the mean of each curve to center them at zero, the evolution of the relative beam centroid position can be seen in Fig. 4. A clear slew is present in the centroid position measurements, which is proportional to the V125

ISBN: 978-3-95450-227-1 ISSN: 2673-5490 doi:10.18429/JACoW-IPAC2022-MOPOPT058

corrector current offset. With these results we can see how both HOM signal peaks and centroid slews are proportional to the corrector current offset (i.e. beam off-axis).

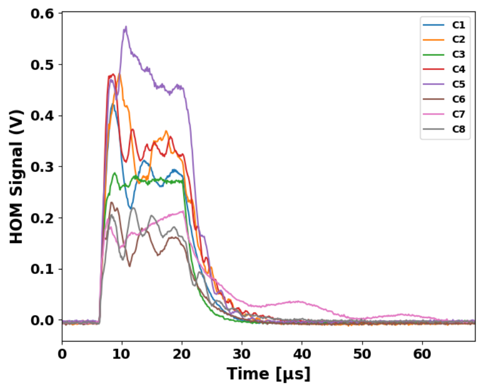

Figure 1: US HOM waveforms for beam of 400 pC/b, V125=1.5 A and H125 at reference value.

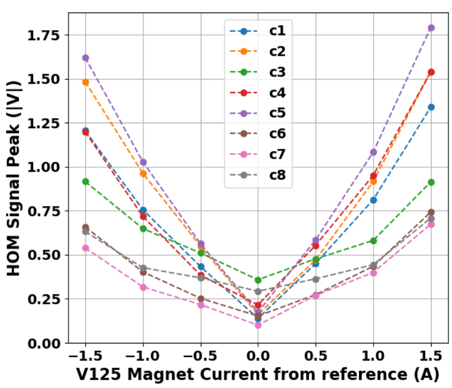

Figure 2: Relation between HOM peak signals average and V125 corrector current with H125 at reference value.

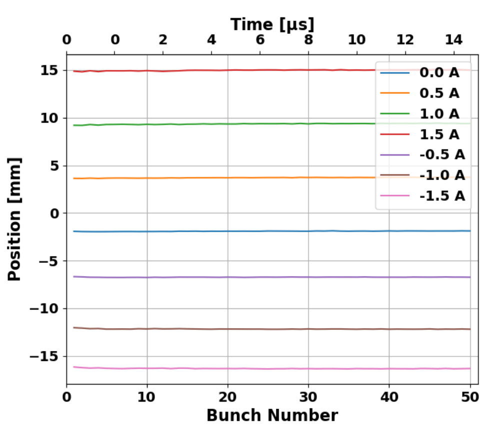

Figure 3: Bunch by bunch BPM mean measurement for B441PV over 300 shots with a beam of 400 pC/b and H125 at reference value.

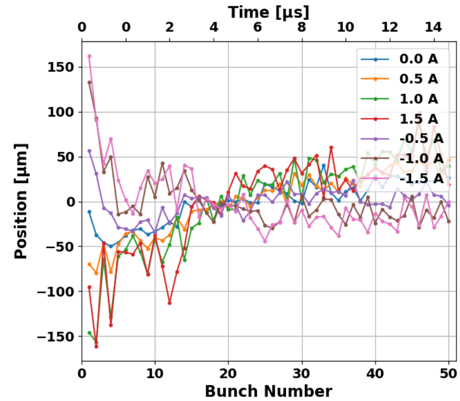

Figure 4: Bunch by bunch centroid slew in B441PV with a beam of 400 pC/b and H125 at reference value.

NEURAL NETWORK MODEL

Two NNs were trained to predict the BPM average measurement and the centroid motion's standard deviation as measured by multiple BPMs for beams with several values of bunch charge and H/V125 corrector currents. The inputs to the NNs are the US and DS HOM signal peaks of 8 cavities. The training data includes measurements for beam charges of 125, 250, 400 and 600 pC/b, V125 corrector currents from -1.5 A to +1.5 A from the reference current, with 0.5 A current steps. At each beam configuration, signals for 300 shots were captured.

The NN architecture for mean prediction has 2 hidden layers each one with 32 nodes, and the NN architecture for centroid motion's standard deviation prediction has 6 hidden layers (four layers of 100 nodes followed by two layers of 64 nodes). Both NNs have a normalization layer and each of its hidden layers uses the hyperbolic tangent activation function. A 80-20 split was used for the training and test datasets. From the training dateset, 20% was used for validation. Early stop was implemented.

TRAINING RESULTS

The performance of the models was evaluated in terms of the mean absolute error (MAE) and the mean absolute percentage error (MAPE). Computing resources of the SLAC Shared Scientific Data Facility (SDF) were used to perform the NN training [5]. The results are shown in Table 1 and Table 2. The error in the prediction of the BPM's mean is less than 1% and the error in the prediction of the standard deviation of the bunch by bunch centroid slew is less than 10% for all BPMs. The performance of the NN model for predictions of B441PV mean over the test dataset is shown in Fig. 5, and the performance of the NN model for predictions of B441PV standard deviation over the test dataset is shown in Fig. 6. Histograms of the test dataset MAPE for B441PV for mean and standard deviation prediction are shown in Fig. 7 and Fig. 8, respectively.

The groups in Figs. 5 and 6 represent BPM measurements over the same beam and corrector configuration (i.e. fixed bunch charge and H/V125 corrector currents). The NN model is capable of predicting the average bunch by bunch centroid slew's standard deviation for a given beam and corrector configuration. However, it is not as accurate when predicting the exact value. This may be related to the noise on the BPM measurements and the low charge. Having the average bunch by bunch centroid slew's standard deviation might be enough when designing a controller based on this predictions.

Table 1: NN Results for BPM Mean Prediction

BPM	**Train MAE [µm]**	**Val MAE [µm]**	**Test MAE [µm]**	**Test MAPE [%]**
B418PV	41.05	40.75	41.03	0.61
B441PV	44.25	42.94	46.69	0.91

Table 2: NN Results for BPM STD Prediction

BPM	**Train MAE [µm]**	**Val MAE [µm]**	**Test MAE [µm]**	**Test MAPE [%]**
B440PV	41.42	41.98	42.82	9.76
B440PH	29.82	30.46	30.54	8.20
B441PV	18.98	19.26	19.50	8.40
B441PH	20.89	21.43	21.62	8.44

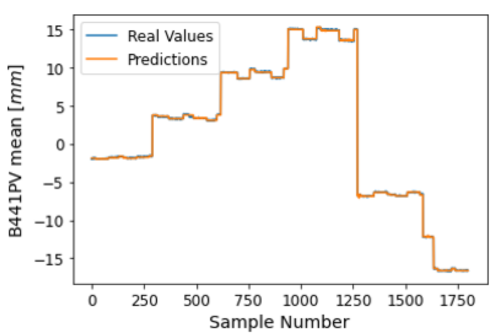

Figure 5: Predictions vs real values of BPM's mean.

CONCLUSIONS

Data with the correlation between beam steering, US and DS HOM signals and BPM measurements showing bunch by bunch centroid slew after a Tesla-type CM at FAST has been used to train NN models. Results show that the NN model is capable of predicting the BPM's mean with an error of less than 1% and the centroid slew's standard deviation with less than 10% error. These are encouraging results towards developing a ML-based controller for HOM reduction for the LCLS-II project at SLAC.

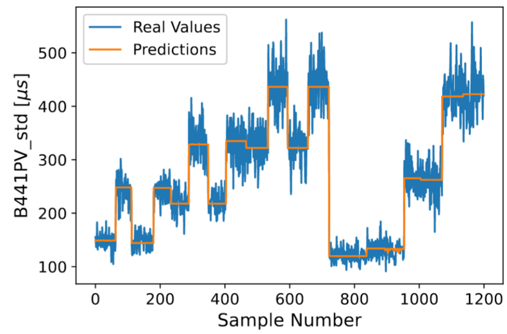

Figure 6: Predictions vs real values of BPM's std.

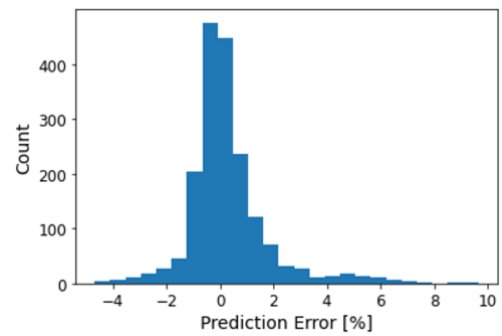

Figure 7: Histogram of mean prediction errors.

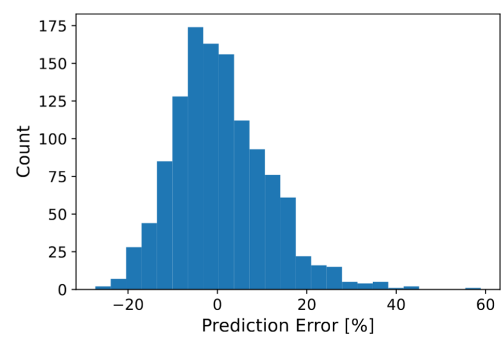

Figure 8: Histogram of standard deviation prediction errors.

ACKNOWLEDGEMENTS

The Fermilab authors acknowledge the support of C. Drennan, A. Valishev, D. Broemmelsiek, G. Stancari, and M. Lindgren, all in the Accelerator Division at Fermilab. The SLAC/FNAL authors acknowledge the support of J. Schmerge (Superconducting Linac Division, SLAC).

REFERENCES

[1] A. H. Lumpkin *et al.*, "Submacropulse electron-beam dynamics correlated with higher-order modes in Tesla-type superconducting rf cavities", *Phys. Rev. Accel. Beams*, vol. 21, no. 6, p. 064401, 2018. doi:10.1103/PhysRevAccelBeams.21.064401

[2] A. H. Lumpkin *et al.*, "Submicropulse electron-beam dynamics correlated with short-range wakefields in Tesla-type superconducting rf cavities", *Phys. Rev. Accel. Beams*, vol. 23, no. 5,

ISBN: 978-3-95450-227-1 ISSN: 2673-5490 doi:10.18429/JACoW-IPAC2022-MOPOPT058

p. 054401, 2020. doi:10.1103/PhysRevAccelBeams.23.054401

[3] J. P. Sikora *et al.*, “Commissioning of the LCLS-II Prototype HOM Detectors with Tesla-Type Cavities at Fast”, in *Proc. IPAC’21*, Campinas, Brazil, May 2021, pp. 996–999. doi:10.18429/JACoW-IPAC2021-MOPAB323

[4] A. H. Lumpkin *et al.*, “Investigations of Long-Range Wakefield Effects in a TESLA-type Cryomodule at FAST”, in *Proc. IPAC’21*, Campinas, Brazil, May 2021, pp. 2109–2112. doi:10.18429/JACoW-IPAC2021-TUPAB274

[5] SLAC Shared Scientific Data Facility, https://ondemand-dev.slac.stanford.edu/.